IOP Publishing | Royal Swedish Academy of Sciences Physica Scripta

Phys. Scr. 90 (2015) 045210 (12pp) doi:10.1088/0031-8949/90/4/045210

# A secure communication scheme based generalized function projective synchronization of a new 5D hyperchaotic system

**Xiangjun Wu[1,2,3], Zhengye Fu[1] and Jürgen Kurths[2,3]**

[1] College of Software, Henan University, Kaifeng 475004, People's Republic of China
[2] Potsdam Institute for Climate Impact Research (PIK), D-14473 Potsdam, Germany
[3] Department of Physics, Humboldt University, D-12489 Berlin, Germany

E-mail: xiangjung.wu@gmail.com

Received 19 October 2014, revised 3 January 2015
Accepted for publication 30 January 2015
Published 27 March 2015

**Abstract**

In this paper, a new five-dimensional hyperchaotic system is proposed based on the Lü hyperchaotic system. Some of its basic dynamical properties, such as equilibria, Lyapunov exponents, bifurcations and various attractors are investigated. Furthermore, a new secure communication scheme based on generalized function projective synchronization (GFPS) of this hyperchaotic system with an uncertain parameter is presented. The communication scheme is composed of the modulation, the chaotic receiver, the chaotic transmitter and the demodulation. The modulation mechanism is to modulate the message signal into the system parameter. Then the chaotic signals are sent to the receiver via a public channel. In the receiver end, by designing the controllers and the parameter update rule, GFPS between the transmitter and receiver systems is achieved and the unknown parameter is estimated simultaneously. The message signal can be finally recovered by the identified parameter and the corresponding demodulation method. There is no any limitation on the message size. Numerical simulations are performed to show the validity and feasibility of the presented secure communication scheme.

Keywords: five-dimensional (5D) hyperchaotic system, Lü hyperchaotic system, generalized function projective synchronization (GFPS), secure communication, parameter estimation, message size

(Some figures may appear in colour only in the online journal)

## 1. Introduction

It is well known that there is at least one positive Lyapunov exponent in chaotic systems. However, in the case where there is just one positive Lyapunov exponent, the system is not safe enough to mask messages [1]. Higher-dimensional hyperchaotic systems are often recommended for addressing this issue. Hyperchaos is characterized as a chaotic system with more than one positive Lyapunov exponent, indicating that its dynamics are expanded in more than one direction simultaneously, which can increase randomness and unpredictability. Because of its higher unpredictability than simple chaotic systems, hyperchaotic systems may be more useful in some fields such as secure communication, encryption, etc. In recent years, many hyperchaotic systems have been developed numerically and experimentally by adding a simple state feedback controller or a sinusoidal parameter perturbation controller in the generalized Lorenz system, Chen system, Lü system and a unified chaotic system [2, 3]. It was also noticed that hyperchaos can be generated based on lower-dimensional chaotic systems by employing an additional state input [4, 5]. Up to now, almost all hyperchaotic systems are four-dimensional systems, which have double-wing hyperchaotic attractors with three or five equilibrium points [6, 7].

 

Generating a hyperchaotic attractor from a smooth dynamical system with only one equilibrium point is a very rare phenomenon [8]. Motivated by the above discussions, this paper presents a new five-dimensional (5D) hyperchaotic system with only one equilibrium point, which is generated from the 4D Lü hyperchaotic system. The hyperchaotic dynamic behavior of the new system is demonstrated by computer simulations.

Since the seminal work of Pecora and Carrol [9], synchronization of chaotic systems for secure communication has received much attention [10–15]. So far, various types of synchronization phenomena in the chaotic systems have been reported, such as complete synchronization [9], generalized synchronization [16], phase synchronization [17], lag synchronization [18], projective synchronization [10] etc. Recently, the concept of function projective synchronization (FPS) has been introduced [19–21], where the drive and response systems could be synchronized up to a scaling function. Du *et al* [22] presented a new type of synchronization, the modified function projective synchronization, where the drive and response systems could be synchronized up to a desired scaling function matrix. Yu and Li [23] studied adaptive generalized function projective synchronization between two different uncertain chaotic systems. In the application to secure communication, the scaling function matrix may also be a useful utility to improve the security of the secure communication scheme. Therefore, it is essential to study FPS of hyperchaotic systems and its application to secure communication.

The general idea for transmitting a message via chaotic systems is that a message signal is embedded in the transmitter system which produces a chaotic signal. The chaotic signal is emitted to the receiver through a public channel. Finally, the message signal is recovered by the receiver. In recent years, many types of secure communication schemes have been presented [24, 25]. The techniques of chaotic communication can be divided into three categories: chaos masking [11, 12], chaos modulation [26–28] and chaos shift keying [29, 30]. In chaotic masking, the message signal is added to a chaotic signal and the combined signal is then transmitted to the receiver. The message can be extracted under certain conditions in the receiver terminal. In chaotic modulation, the message is injected into the states or the parameters of the chaotic system, or is modulated by using an invertible transformation. If the transmitter and the receiver are synchronized, the message signal can be recovered by a receiver. In chaos shift keying, we assume that the message is binary, and it is mapped into the transmitter and the receiver. The message signal can be recovered by a receiver as synchronization between the transmitter and the receiver occurs. To our knowledge, in most of secure communication schemes [10–13, 24, 27], the message size is required to be sufficiently small, otherwise it may induce a chaotic system to be asymptotically stable or emanative, which may render the failure of recovering the emitted signal. In addition, another method considered in [26, 28] is that the upper and lower bounds of the message signal must be known in advance. However, in real situations, some messages to be transmitted may be very large or unbounded. For example, the messages are $t^2$, $e^t$, $t\sin(t)$ etc, $t < \infty$. The existing secure communication methods are clearly invalid for unbounded messages. Recently, chaotic complex systems are attempted to apply for secure communications because doubling the number of variables increases the content and security of the transmitted information [31, 32]. Mahmoud *et al* [31] transmitted more than one large or bounded message by the passive projective synchronization of uncertain hyperchaotic complex nonlinear system. Liu and zhang [32] proposed a secure communication scheme based on complex function projective synchronization of complex chaotic systems and chaotic masking. However, there are defects in their method such as complex controllers, high control cost and only applying to bounded or very small signals. So it is an important issue to investigate how to transmit unbounded message signals.

In this work, a new secure communication scheme is introduced based on generalized function projective synchronization (GFPS) of the novel 5D hyperchaotic system and parameter modulation. The message signal to be emitted may be bounded or unbounded. In the transmitter side, the message signal is firstly modulated by an invertible function. Then this modulated signal is taken as the parameter of the 5D hyperchaotic system to guarantee communication security. We only transmit the unpredictable chaotic states through a public channel to the receiver. Suppose that the parameter of the receiver system is unknown. In the receiver end, the controllers and corresponding parameter update rule are designed to achieve GFPS between the transmitter and receiver systems and estimate the unknown parameter simultaneously. Finally, the original message signal transmitted from the transmitter can be successfully recovered by the estimated parameter and the presented invertible function. Simulation results show the effectiveness and feasibility of the proposed communication scheme.

The rest of this paper is organized as follows. In section 2, a new 5D hyperchaotic system is generated from the Lü hyperchaotic system. The properties and dynamics of the hyperchaotic system are investigated numerically. In section 3, a secure communication scheme via GFPS of the 5D hyperchaotic system with uncertain parameter is proposed. The controllers and the parameter update rule are devised for obtaining the desired synchronization and identify the unknown parameter simultaneously. Numerical simulations are given to illustrate and validate the proposed communication scheme in section 4. Our conclusions are finally drawn in section 5.

## 2. Generation and dynamical analysis of a new 5D hyperchaotic system

Based on the original Lü chaotic system, the Lü hyperchaotic system was constructed by employing a feedback controller

[33], which is described by

$$\begin{cases} \dot{x} = a(y - x) + w, \\ \dot{y} = -xz + cy, \\ \dot{z} = xy - bz, \\ \dot{w} = xz + dw, \end{cases} \quad (1)$$

where $x$, $y$, $z$ and $w$ are state variables and $a$, $b$, $c$, $d$ are real constant parameters. When $a = 36$, $b = 3$, $c = 20$ and $-0.35 \leqslant d \leqslant 1.3$, the system (1) exhibits a hyperchaotic behavior.

By eliminating the linear feedback controller from the first equation and introducing a linear feedback controller to the second one of system (1), a new 5D hyperchaotic system can be obtained as follows:

$$\begin{cases} \dot{x} = a(y - x), \\ \dot{y} = -xz + cy + v, \\ \dot{z} = xy - bz, \\ \dot{w} = xz + dw, \\ \dot{v} = -x - y, \end{cases} \quad (2)$$

where $a$, $b$, $c$ and $d$ are again system parameters and $d \leqslant 0$.

### 2.1. Symmetry

System (2) is symmetric respect to the $z$-axis, i.e., it is invariant under the following coordinate transformations $(x, y, z, w, v) \to (-x, -y, z, -w, -v)$.

### 2.2. Dissipation

The divergence of the system (2) is

$$\nabla V = \frac{\partial \dot{x}}{\partial x} + \frac{\partial \dot{y}}{\partial y} + \frac{\partial \dot{z}}{\partial z} + \frac{\partial \dot{w}}{\partial w} + \frac{\partial \dot{v}}{\partial v} = -a + c - b + d = -19 + d.$$

Obviously, for the parameter values considered here, we get $-19 + d < 0$, i.e., system (2) is dissipative. Hence, the new dynamical system (2) converges to a set of measure zero exponentially, i.e., $\dot{V}(t) = \mathrm{e}^{-19+d}$. It indicates that $V(t) = V_0(t)\mathrm{e}^{(-19+d)t}$ for any initial cubage $V_0(t)$, and the orbit flows into a certain bounded region as $t \to \infty$.

### 2.3. Equilibria and stability

The equilibria of system (2) can be obtained by solving the following equations:

$$a(y - x) = 0,\ -xz + cy + v = 0, xy - bz = 0,\ xz + dw = 0,\ -x - y = 0. \quad (3)$$

It is easy to find that system (2) has only one trivial equilibrium point $E_0(0,0,0,0,0)$. By linearizing system (2) around $E_0$, we yield the following Jacobian matrix:

$$J = \begin{pmatrix} -a & a & 0 & 0 & 0 \\ 0 & c & 0 & 0 & 1 \\ 0 & 0 & -b & 0 & 0 \\ 0 & 0 & 0 & d & 0 \\ -1 & -1 & 0 & 0 & 0 \end{pmatrix}.$$

The corresponding characteristic equation is:

$$\lambda(\lambda + b)(\lambda - d)\left[\lambda^2 + (a - c)\lambda - ac + 1\right] = 0. \quad (4)$$

For $a = 36, b = 3, c = 20$ and $d \leqslant 0$, the eigen values of the Jacobian matrix $J$ are:

$$\lambda_1 = 20,\ \lambda_2 = 19.98,\ \lambda_3 = 0,\ \lambda_4 = d \text{ and } \lambda_5 = -35.98.$$

Here $\lambda_1$ and $\lambda_2$ are two positive real numbers. If $d < 0$, $\lambda_4$ and $\lambda_5$ are two negative real numbers; otherwise, $\lambda_5$ is a negative real number. Therefore, the equilibrium $E_0(0,0,0,0,0)$ is an unstable saddle point.

### 2.4. Dynamics in the new 5D system

In the following, the basic dynamics of the new 5D system (2) is studied by means of the Lyapunov exponents spectrum and corresponding bifurcation diagrams. We compute the Lyapunov exponents $L_i$ $(i = 1,2,3,4,5)$ by the Wolf algorithm [34]. Some simulations were performed with varying parameters to analyze the dynamics of system (2), and the findings are summarized as follows.

**Case I.** Fix $a = 36,\ b = 3,\ c = 20$ and vary $d$ .

Figure 1(a) displays the Lyapunov exponents spectrum of the 5D system (2) with respect to parameter $d$. Figure 1(b) shows the bifurcation diagram of state $y$ versus parameter $d$. Obviously, when $d \in [-50,0]$, there are $L_1 > 0$, $L_2 > 0$, $L_3 = 0$, $L_4 < 0$ and $L_5 < 0$, which implies that the new system (2) is always hyperchaotic. In order to further observe the new hyperchaotic attractors, some phase portraits of the 5D system (2) with different $d$ are plotted in figure 2.

**Case II**. Fix $b = 3,\ c = 20,\ d = -1$ and vary $a$.

Figure 3 plots the spectrum of Lyapunov exponents and corresponding bifurcation diagram of system (2) with respect to parameter $a$. When $a \in [21,26.4)$, $L_1 = 0$ and $L_\tau < 0$ $(\tau = 2,3,4,5)$, implying that the 5D system (2) is periodic shown in figures 4(a) and (b). As $a \in [26.4,60.2]$, $L_1 > 0$, $L_2 > 0$, $L_3 = 0$, $L_4 < 0$ and $L_5 < 0$, which means that system (2) is hyperchaotic. When $a \in (60.2,61]$, $L_1 > 0$ and $L_\tau < 0$ $(\tau = 2,3,4,5)$, so system (2) is chaotic. As $a \in (61,120]$, $L_1 = 0$ and $L_\tau < 0$ $(\tau = 2,3,4,5)$, indicating that system (2) eventually evolves to a periodic orbit. From the bifurcation diagram shown in figure 3(b), one can clearly see that, starting from the periodic region (for instance, the phase diagrams are shown in figures 4(a) and (b)), with $a$ increasing, the state $y$ goes through a process of hyperchaos (figure 4(c)), chaos and finally to the periodic orbit

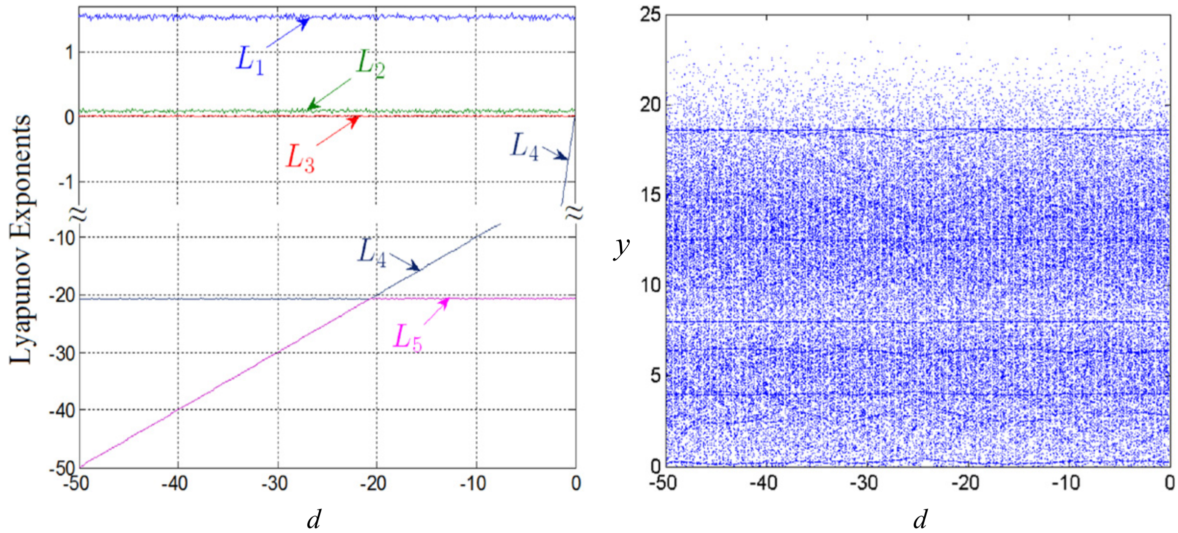


(a) Lyapunov exponents spectrum (b) Bifurcation diagram of $y$

**Figure 1.** Lyapunov exponents spectrum and bifurcation diagram of system (2) with $a = 36$, $b = 3$, $c = 20$, $d \in [-50,\ 0]$.

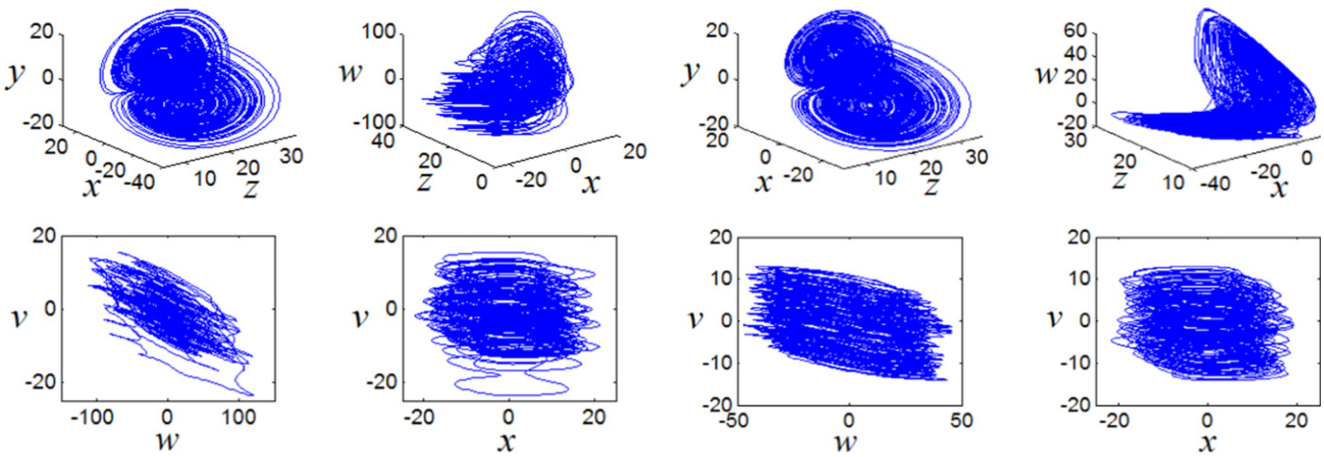

(a) $d = -1$ (b) $d = -5$

**Figure 2.** Phase portraits of the hyperchaotic system (2) with different $d$.

(figure 4(d)).

**Case III**. Fix $a = 36,\ c = 20,\ d = -1$ and vary $b$.

When the parameters $a = 36$, $c = 20$ and $d = -1$ are fixed while parameter $b$ is varied, the spectrum of Lyapunov exponents and the corresponding bifurcation diagram of state $y$ versus $b$ are shown in figure 5. As $b \in [0,0.24)$, $b \in (13.3,15.7]$, $b \in [16.03,16.15]$, $b \in [16.35,16.42)$, $b \in (16.65,17.56)$, $b \in [17.84,17.92]$, $b \in [18.2,18.44]$, $b \in [19,19.1]$, $b \in (19.48,19.52]$ and $b \in [19.68,19.76]$, the maximum Lyapunov exponent $L_1$ equals zeros and other four Lyapunov exponents are negative, representing that system (2) has a periodic orbit. When $b \in [0.24,0.58]$, $b \in [0.61,0.66]$, $b \in (6.2,13.3]$, $b \in (15.7,16.03)$, $b \in (16.15,16.35)$, $b \in [16.42,16.65]$, $b \in [17.56,17.84)$, $b \in (17.92,18.2)$, $b \in (18.44,19)$, $b \in (19.1,19.48]$, $b \in (19.52,19.68)$ and $b \in (19.76,20]$, only $L_1 > 0$, implying that system (2) is chaotic. When $b \in (0.58,0.61)$ and $b \in (0.66,6.2]$, the Lyapunov exponents $L_1$ and $L_2$ are positive, which means that system (2) is hyperchaotic. Figure 5 reveals that periodic orbit, chaos and hyperchaos appear alternately with $b$ increasing gradually from 0 to 20.

**Case IV**. Fix $a = 36,\ b = 3,\ d = -1$ and vary $c$.

In this case, we fix $a = 36$, $b = 3$, $d = -1$ and only change $c$. Figure 6 shows the Lyapunov exponents spectrum and the bifurcation diagram with respect to parameter $c$. When $c \in [0,11.8)$ and $c \in (29.24,30]$, system (2) is periodic, in which the maximum Lyapunov exponent $L_1$ equals zero; while $c \in [11.8,24.78]$, $c \in (24.88,26.5]$, $c \in (27.35,28.08)$, $c \in (28.5,28.8]$ and $c \in (29,29.1]$, system (2) has two positive Lyapunov exponents, implying that it is a hyperchaotic system. When $c \in (24.78,24.88]$, $c \in (26.5,27.35]$, $c \in [28.08,28.5]$, $c \in (28.8,29]$ and $c \in (29.1,29.24]$, system (2) has a single positive Lyapunov exponent, which means that this system has a chaotic orbit. Figure 6(b) displays clearly the whole evolution process of

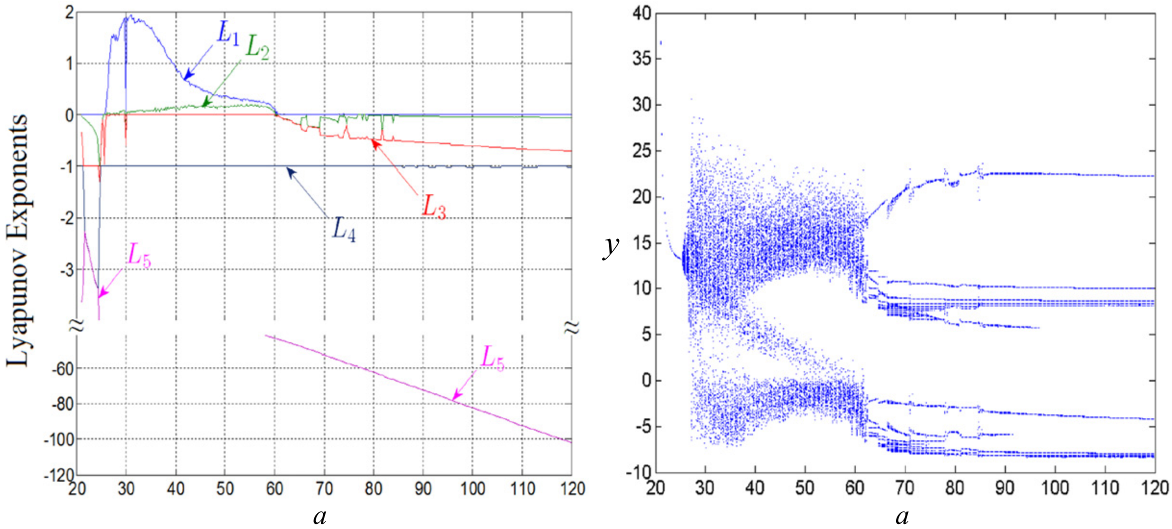


(a) Lyapunov exponents spectrum (b) Bifurcation diagram of $y$

**Figure 3.** Lyapunov exponents spectrum and bifurcation diagram of system (2) with $b = 3$, $c = 20$, $d = -1$, $a \in [21,\ 120]$.

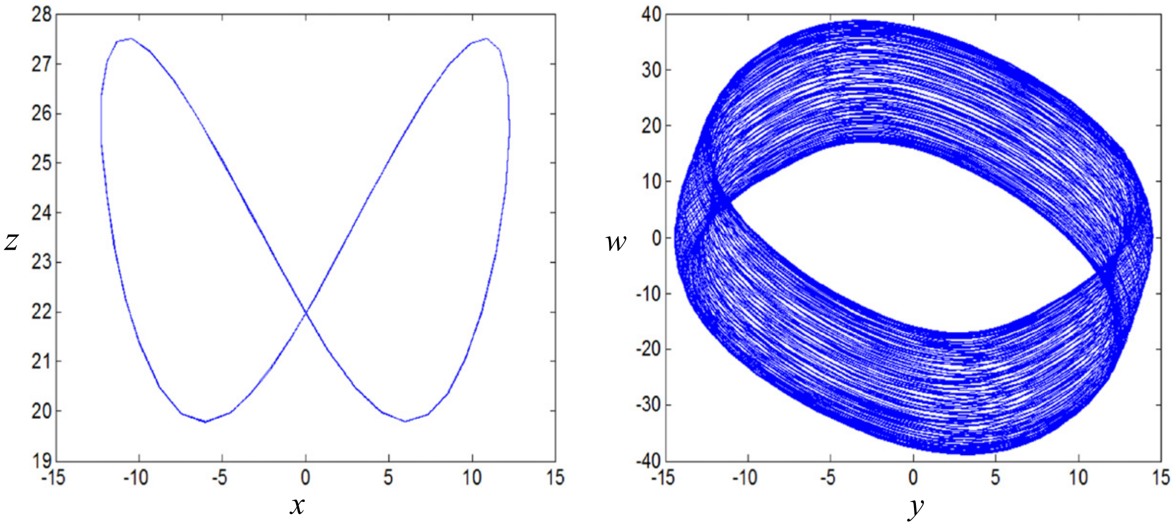


(a) $a = 24.5$ (b) $a = 25.5$

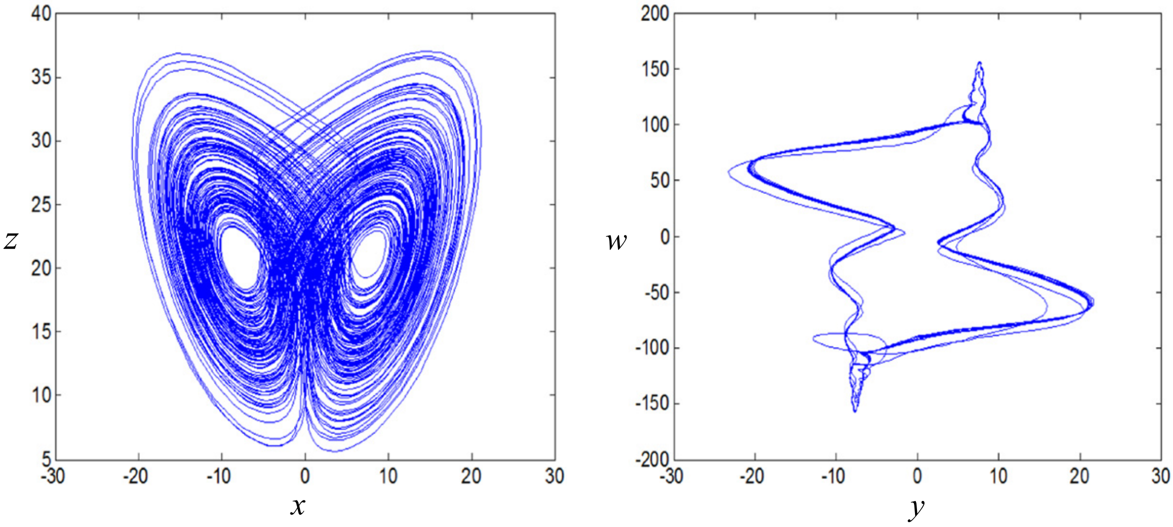


(c) $a = 40$ (d) $a = 72$

**Figure 4.** Phase diagrams of the 5D system (2) with different $a$.

system (2), i.e., from period to hyperchaos, chaos and finally to period again.

## 3. A new secure communication scheme via GFPS of the uncertain 5D hyperchaotic system

In this section, we will introduce a new secure communication method based on GFPS of the new 5D hyperchaotic system (2) with unknown parameter $d$. Figure 7 describes the proposed communication system consisting of a modulation, a transmitter (drive), a receiver (response) at the receiving end of the communication, and a demodulation. The message signal to be transmitted is modulated into the parameter of the chaotic transmitter system by employing an invertible function, and the resulting system is still hyperchaotic. The resulting chaotic signals are sent to the receiver end through a public channel. In the receiver side, by designing suitable controllers, the desired synchronization between the transmitter and receiver systems can be obtained, and the unknown parameter can also be identified at the same time. Then the message signal can be recovered from the estimated parameter by performing the proposed demodulation method. In the following, we will illustrate the secure communication system via GFPS of the new 5D hyperchaotic system with unknown parameter in detail.

### *3.1. Modulation*

For transmitting an arbitrary continuous-time message signal regardless of its size, we consider modulating it into the parameter $d$ of system (2). Let $s(t)$ represent the message signal. Suppose $d_1 \leqslant d \leqslant d_2$, where $d_1 = -1$ and $d_2 = 0$. Obviously, system (2) is always hyperchaotic in this range. It is known that the arc tangent function satisfies: $\arctan() \in (-0.5\pi, 0.5\pi)$. Let us define a new parameter $\rho(t)$. In order to obtain $\rho(t) \in (-1, 0)$, we present the following modulation technique:

$$\begin{aligned}\rho(t) &= \frac{(d_2 - d_1)}{\pi}\arctan(s(t)) + \frac{(d_1 + d_2)}{2}\\ &= \frac{1}{\pi}\arctan(s(t)) - 0.5. \end{aligned} \tag{5}$$

In the following, we will use $\rho(t)$ as the parameter of system (2), which will be explained in detail later.

### *3.2. Transmitter*

Replacing the parameter $d$ in system (2) with the new parameter $\rho(t)$ obtained in section 3.1, we get

$$\begin{cases}\dot{x}_1 = a(y_1 - x_1),\\ \dot{y}_1 = -x_1 z_1 + c y_1 + v_1,\\ \dot{z}_1 = x_1 y_1 - b z_1,\\ \dot{w}_1 = x_1 z_1 + \rho(t) w_1,\\ \dot{v}_1 = -x_1 - y_1.\end{cases} \tag{6}$$

Since $\rho(t) \in (-1, 0)$, the resulting system (6) is still hyperchaotic. We take system (6) as the transmitter system. $x_1$, $y_1$, $z_1$, $w_1$ and $v_1$ are the chaotic signals and need to be transmitted to the receiver via a public channel. Since system (6) is hyperchaotic, it is hard to extract a message from the signals transmitted in the channel.

### *3.3. Receiver*

Consider the receiver system as follows:

$$\begin{cases}\dot{x}_2 = a(y_2 - x_2) + u_1,\\ \dot{y}_2 = -x_2 z_2 + c y_2 + v_2 + u_2,\\ \dot{z}_2 = x_2 y_2 - b z_2 + u_3,\\ \dot{w}_2 = x_2 z_2 + \hat{\rho}(t) w_2 + u_4,\\ \dot{v}_2 = -x_2 - y_2 + u_5,\end{cases} \tag{7}$$

where $\hat{\rho}(t)$ is the unknown parameter to be estimated, $u_i(t)$ ($i = 1,2,3,4, 5$) are the controllers to be designed. Thus, the control objective is to find $u_i(t)$ and $\hat{\rho}(t)$ such that both the transmitter system and the receiver system achieve GFPS, and $\hat{\rho}(t)$ converges to the actual value of $\rho(t)$.

Let us introduce the following state errors:

$$\begin{cases}e_1 = x_2 - \alpha_1(t) x_1,\\ e_2 = y_2 - \alpha_2(t) y_1,\\ e_3 = z_2 - \alpha_3(t) z_1,\\ e_4 = w_2 - \alpha_4(t) w_1,\\ e_5 = v_2 - \alpha_5(t) v_1,\end{cases} \tag{8}$$

and the parameter estimate error as

$$e_\rho = \hat{\rho}(t) - \rho(t). \tag{9}$$

The time derivative of the error signals (8) is

$$\begin{cases}\dot{e}_1 = \dot{x}_2 - \alpha_1(t)\dot{x}_1 - \dot{\alpha}_1(t) x_1,\\ \dot{e}_2 = \dot{y}_2 - \alpha_2(t)\dot{y}_1 - \dot{\alpha}_2(t) y_1,\\ \dot{e}_3 = \dot{z}_2 - \alpha_3(t)\dot{z}_1 - \dot{\alpha}_3(t) z_1,\\ \dot{e}_4 = \dot{w}_2 - \alpha_4(t)\dot{w}_1 - \dot{\alpha}_4(t) w_1,\\ \dot{e}_5 = \dot{v}_2 - \alpha_5(t)\dot{v}_1 - \dot{\alpha}_5(t) v_1.\end{cases} \tag{10}$$

Substituting equations (6) and (7) into equation (10), we have

$$\begin{cases}\dot{e}_1 = -a e_1 + a y_2 - a\alpha_1(t) y_1 - \dot{\alpha}_1(t) x_1 + u_1,\\ \dot{e}_2 = c e_2 - x_2 z_2 + \alpha_2(t) x_1 z_1 + v_2 - \alpha_2(t) v_1\\ \qquad - \dot{\alpha}_2(t) y_1 + u_2,\\ \dot{e}_3 = -b e_3 + x_2 y_2 - \alpha_3(t) x_1 y_1 - \dot{\alpha}_3(t) z_1 + u_3,\\ \dot{e}_4 = \hat{\rho} e_4 + \alpha_4(t) e_\rho w_1 + x_2 z_2 - \alpha_4(t) x_1 z_1\\ \qquad - \dot{\alpha}_4(t) w_1 + u_4,\\ \dot{e}_5 = -x_2 - y_2 + \alpha_5(t) x_1 + \alpha_5(t) y_1 - \dot{\alpha}_5(t) v_1 + u_5.\end{cases} \tag{11}$$

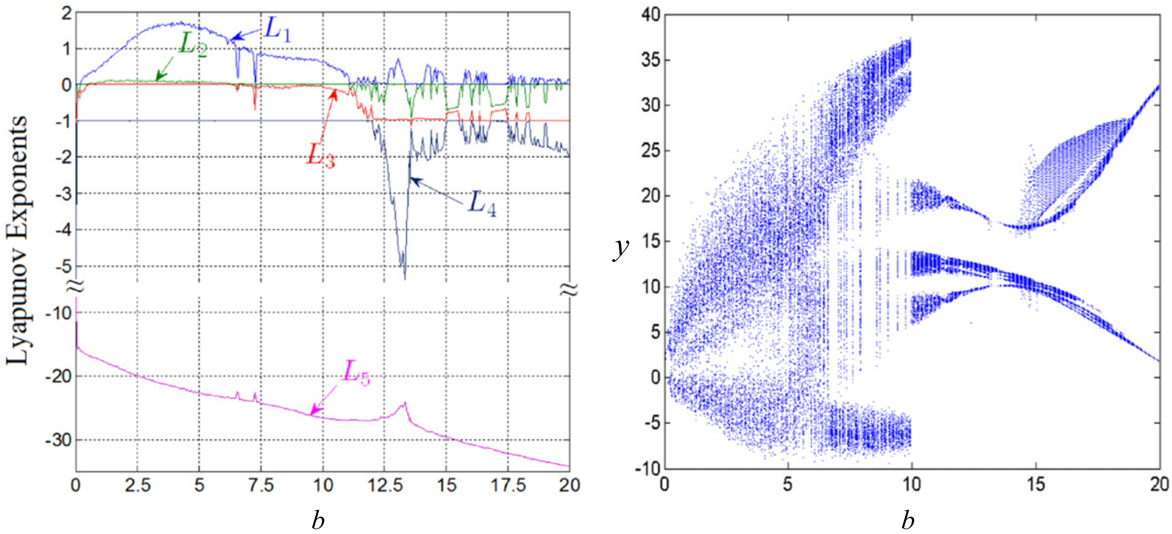


(a) Lyapunov exponents spectrum (b) Bifurcation diagram of $y$

**Figure 5.** Lyapunov exponents spectrum and bifurcation diagram of system (2) with $a = 36$, $c = 20$, $d = -1$, $b \in [0,\ 20]$.

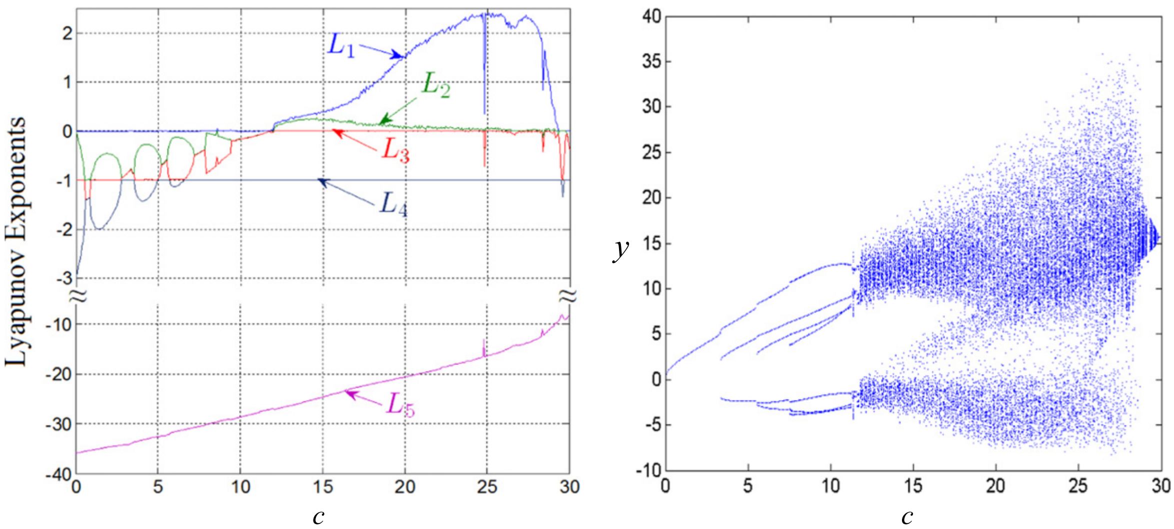


(a) Lyapunov exponents spectrum (b) Bifurcation diagram of $y$

**Figure 6.** Lyapunov exponents spectrum and bifurcation diagram of system (2) with $a = 36$, $b = 3$, $d = -1$, $c \in [0,\ 30]$.

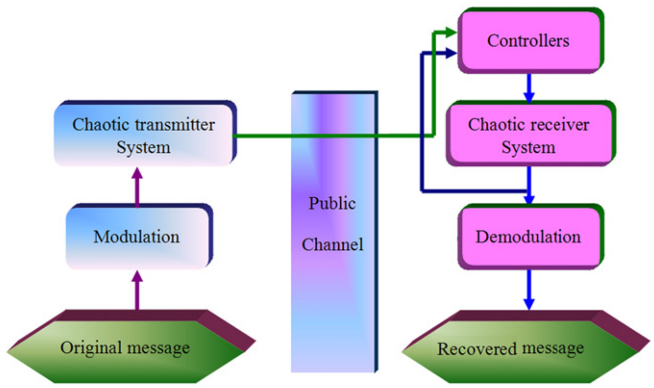


**Figure 7.** Block diagram of the proposed secure communication system.

Taking the time derivative on both sides of equation (9) yields

$$\dot{e}_\rho = \dot{\hat{\rho}}(t) - \frac{\dot{s}(t)}{\pi\left(1 + s^2(t)\right)}. \tag{12}$$

Hence the synchronization problem becomes the stability problem of the error dynamics (11).

We get the following main theorem.

**Theorem 1.** *For given nonzero scaling functions* $\alpha_i(t)$ $(i = 1,2,3,4,\ 5)$, *GFPS between the transmitter (6) and the receiver system (7) can be achieved, and the uncertain parameter* $\hat{\rho}(t)$ *can be estimated, if the controllers and the parameter update rule are constructed as follows:*


**Figure 8.** Hardware architecture of implementing arctan function.

$$\begin{cases} u_1 = -ay_2 + a\alpha_1(t)y_1 \\ \quad + \dot{\alpha}_1(t)x_1 - k_1e_1, \\ u_2 = x_2z_2 - \alpha_2(t)x_1z_1 \\ \quad - v_2 + \alpha_2(t)v_1 \\ \quad + \dot{\alpha}_2(t)y_1 - k_2e_2, \\ u_3 = -x_2y_2 + \alpha_3(t)x_1y_1 \\ \quad + \dot{\alpha}_3(t)z_1 - k_3e_3, \\ u_4 = -x_2z_2 + \alpha_4(t)x_1z_1 \\ \quad + \dot{\alpha}_4(t)w_1 - \left(k_4 + \hat{\rho}\right)e_4, \\ u_5 = x_2 + y_2 - \alpha_5(t)x_1 \\ \quad - \alpha_5(t)y_1 + \dot{\alpha}_5 \\ \quad \times (t)v_1 - k_5e_5, \end{cases} \tag{13}$$

and

$$\dot{\hat{\rho}}(t) = -\alpha_4(t)w_1e_4 + \frac{\dot{s}(t)}{\pi\left(1 + s^2(t)\right)}, \tag{14}$$

respectively, where $k_i$ $(i = 1,2,3,4,5)$ are positive control gains and $k_2 > c$.

**Proof.** Choose the following Lyapunov function candidate:

$$V(t) = \frac{1}{2}\left(e_1^2 + e_2^2 + e_3^2 + e_4^2 + e_5^2 + e_\rho^2\right). \tag{15}$$

By calculating the derivative of $V(t)$ along the trajectories of the error system (11), and using equations (13) and (14), we have

$$\begin{aligned} \dot{V}(t) &= e_1\dot{e}_1 + e_2\dot{e}_2 + e_3\dot{e}_3 + e_4\dot{e}_4 + e_5\dot{e}_5 + e_\rho\dot{e}_\rho \\ &= e_1\left[-ae_1 + ay_2 - a\alpha_1(t)y_1 - \dot{\alpha}_1(t)x_1 + u_1\right] \\ &\quad + e_2\left[ce_2 - x_2z_2 + \alpha_2(t)x_1z_1 + v_2 - \alpha_2(t)v_1 \right.\\ &\quad \left. - \dot{\alpha}_2(t)y_1 + u_2\right] \\ &\quad + e_3\left[-be_3 + x_2y_2 - \alpha_3(t)x_1y_1 - \dot{\alpha}_3(t)z_1 + u_3\right] \\ &\quad + e_4\left[\hat{\rho}e_4 + \alpha_4(t)e_\rho w_1 + x_2z_2 - \alpha_4(t)x_1z_1 \right.\\ &\quad \left. - \dot{\alpha}_4(t)w_1 + u_4\right] \\ &\quad + e_5\left[-x_2 - y_2 + \alpha_5(t)x_1 + \alpha_5(t)y_1 \right.\\ &\quad \left. - \dot{\alpha}_5(t)v_1 + u_5\right] \\ &\quad + e_\rho\left[\dot{\hat{\rho}}(t) - \dot{s}(t)\big/\pi\left(1 + s^2(t)\right)\right] \\ &= -\left(a + k_1\right)e_1^2 - \left(k_2 - c\right)e_2^2 - \left(b + k_3\right) \\ &\quad \times e_3^2 - k_4e_4^2 - k_5e_5^2 < 0. \end{aligned}$$

Obviously, $V(t)$ is positive definite and $\dot{V}(t)$ is negative definite. By the Lyapunov stability theorem, the synchronization errors $e_i$ $(i = 1,2,3,4,5)$ asymptotically converge to zero, i.e., GFPS between the transmitter system (6) and the receiver system (7) is obtained, and the zero point of the parameter error $e_\rho$ is globally and asymptotically stable. It implies that the uncertain parameter $\rho(t)$ is also estimated in the receiver simultaneously. This completes the proof. □

### *3.4. Demodulation*

As GFPS between the transmitter and receiver systems appears, one can identify the parameter $\hat{\rho}(t)$ based on theorem 2. According to the invertible transformation function (5), the original message signal can be recovered as

$$\hat{s}(t) = \tan\left(\pi\left(\hat{\rho}(t) + 0.5\right)\right). \tag{16}$$

Here $\hat{s}(t)$ represents the recovered signal. When the desired synchronization takes place, we have $\hat{\rho}(t) \to \rho(t)$ as $t \to \infty$. One further gets

$$\hat{s}(t) = \tan\left(\pi\left(\hat{\rho}(t) + 0.5\right)\right) \to s(t) = \tan(\pi(\rho(t) + 0.5))$$

as $t \to \infty$. Therefore, the receiver can extract the message signal successfully from $\hat{\rho}(t)$ by the above modulation method.

**Remark 1.** The cordinate rotation digital computer (CORDIC) algorithm is traditionally used for the implementation of trigonometric functions. Besides general scientific and technical computation, the CORDIC algorithm has been utilized for various applications such as signal and image processing, communication systems and robotics [35–38]. In practical engineering, the arctan and tangent functions can be implemented based on the CORDIC algorithm. The hardware architectures of implementing arctan function and tangent function are shown in figures 8 and 9, respectively.

**Remark 2.** In figure 8, the inputs $\chi_1, \chi_2 \in (-\infty, +\infty)$ are IEEE 754 standard single precision floating point numbers. The floating point numbers $\chi_1$ and $\chi_2$ are firstly preprocessed in the input data format transform unit to obtain two fixed point integer numbers, i.e., $\bar{\chi}_1$ and $\bar{\chi}_2$, where $\bar{\chi}_1, \bar{\chi}_2 \in [-1, +1]$. $\bar{\chi}_1$ and $\bar{\chi}_2$ are considered as the inputs of CORDIC unit. Next, the CORDIC algorithm is employed to compute the arctan function by using $\bar{\chi}_1$ and $\bar{\chi}_2$, and one can get the result $\mu$. The CORDIC algorithm has been implemented by many ways with software and hardware [36, 38]. Finally, in the output data format transform unit, we convert the fixed point integer number $\mu$ into the IEEE 754 standard single precision floating point number $\bar{\mu}$. Corresponding software simulation and hardware experiment can be conducted on FPGAs [39].

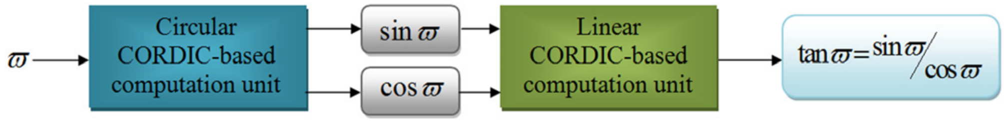


**Figure 9.** Hardware architecture of implementing tangent function.

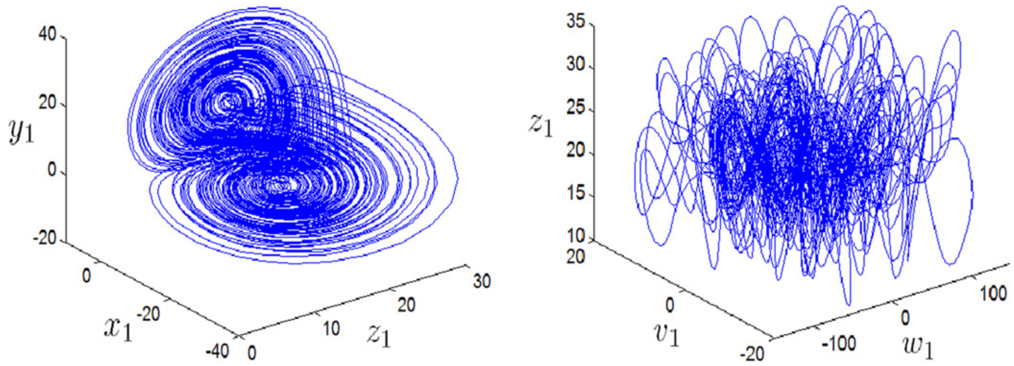

**Figure 10.** The hyperchaotic attractors of the resulting system (6).

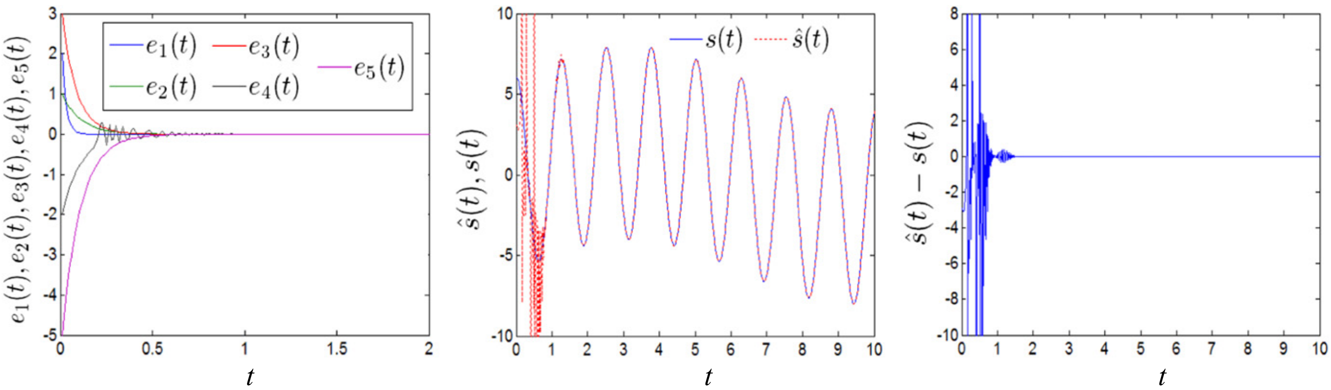

(a) Synchronization errors (b) The original and recovered signals (c) The error signal $\hat{s}(t) - s(t)$

**Figure 11.** Simulation results of secure communication based on GFPS of the 5D hyperchaotic system when the information signal is a bounded signal $s(t) = 2\ \sin(0.5t) + 6\ \cos(5t)$.

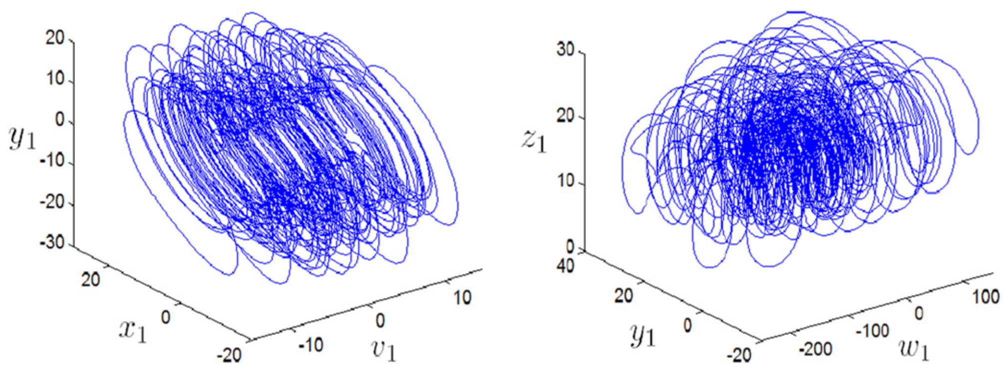

**Figure 12.** The hyperchaotic attractors of the resulting system (6).

**Remark 3.** In figure 9, the circular CORDIC algorithm is firstly applied to get two results, i.e., $\sin\varpi$ and $\cos\varpi$, with the input $\varpi$. Then we use $\sin\varpi$ and $\cos\varpi$ as the inputs of the linear CORDIC-based computation unit, and the value of $\tan\varpi$ can be obtained by means of the linear CORDIC algorithm. The implementation of the circular CORDIC algorithm has been reported in the literature [37, 39–41]. The linear CORDIC algorithm only involves with addition and shift operations, which makes it very convenient implement on the hardware.

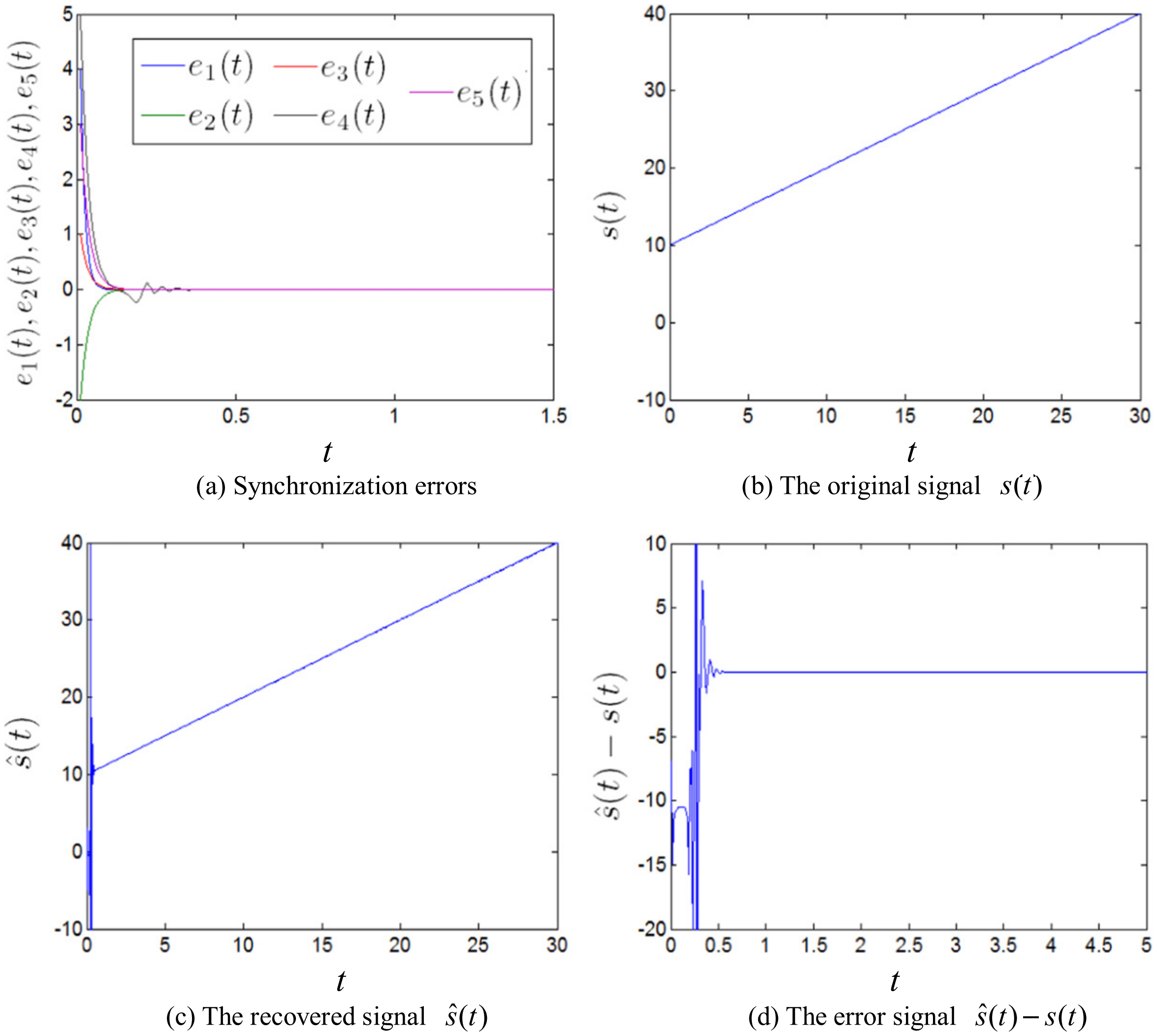


**Figure 13.** Simulation results of secure communication based on GFPS of the 5D hyperchaotic system when the information signal is an unbounded signal $s(t) = 10 + t$.

## 4. Simulation results

In this section, computer simulations are performed to show the efficiency of the proposed communication system. The ODE45 algorithm is adopted to solve the differential equations. The system parameters are set as $a = 36$, $b = 3$ and $c = 20$. In the following simulations, for saving space, we consider two cases: (i) choose a bounded message signal for secure communication; (ii) choose an unbounded message signal for secure communication.

### 4.1. A bounded information signal for secure communication

Here the message signal hidden in the transmitter system is $s(t) = 2\sin(0.5t) + 6\cos(5t)$. Obviously, $|s(t)| \leqslant 8$. By equation (5), $\rho(t)$ can be obtained as follows:

$$\rho(t) = \frac{1}{\pi}\arctan(2\sin(0.5t) + 6\cos(5t)) - 0.5. \quad (17)$$

The initial conditions for the transmitter system (6) and the receiver system (7) are arbitrarily chosen as $x_1(0) = -2$, $y_1(0) = 1$, $z_1(0) = 3$, $w_1(0) = 0$ and $v_1(0) = 4$; $x_2(0) = -5$, $y_2(0) = 0$, $z_2(0) = 2$, $w_2(0) = -1$ and $v_2(0) = 3$, respectively. The initial value of the unknown parameter $\hat{\rho}(t)$ is taken as $\hat{\rho}(0) = -0.1$. Let the control gains be $k_1 = k_3 = k_4 = k_5 = 10$ and $k_2 = 30$. The scaling functions are selected randomly as $\alpha_1(t) = v_1(t)$, $\alpha_2(t) = \cos(t) - 3$, $\alpha_3(t) = z_1(t) + 1$, $\alpha_4 = \sin(10t) - 3\cos(2t) + 5$ and $\alpha_5 = 8 - 5\sin(0.2t)$.

Figure 10 displays the hyperchaotic behavior of the resulting system (6). The simulation results of the proposed secure communication system are given in figure 11. In figure 11(a), we see that the synchronization errors $e_i$ ($i = 1,2,3,4,5$) asymptotically converge to zero quickly. That is, GFPS between the transmitter system and the uncertain receiver system is achieved under the controllers (13) and the parameter update rule (14). Figure 11(b) depicts the original message signal $s(t)$ (blue and solid line) and the recovered signal $\hat{s}(t)$ (red and dotted line) via the demodulator (16). It is easily seen that the reconstructed signal $\hat{s}(t)$ coincides with the message signal $s(t)$ with good accuracy. This can be further validated by figure 11(c) which shows the message signal recovery error $\hat{s}(t) - s(t)$. As expected, the signal recovery error quickly converges to zero and the communication goal is attained.

### 4.2. An unbounded information signal for secure communication

In this section, we simulate the presented secure communication system with an unbounded message signal. For example, the message signal $s(t) = 10 + t$, where $|s(t)| < \infty$. From equation (5), we get

$$\rho(t) = \frac{1}{\pi} \arctan(10 + t) - 0.5. \tag{18}$$

Corresponding initial values are arbitrarily set as follows: $x_1(0) = 3$, $y_1(0) = 2$, $z_1(0) = -1$, $w_1(0) = 2$, $v_1(0) = 5$, $x_2(0) = 2$, $y_2(0) = -4$, $z_2(0) = -3$, $w_2(0) = 5$, $v_2(0) = 0$ and $\hat{\rho}(0) = -0.1$. The control gains are given as $k_1 = k_3 = k_4 = k_5 = 40$ and $k_2 = 60$. We randomly choose the scaling functions as $\alpha_1(t) = 6 + 2\sin(0.5t)$, $\alpha_2(t) = 2+3\cos(t)$, $\alpha_3(t) = 2\sin(t) - 1$, $\alpha_4 = -2$ and $\alpha_5 = 2 - \sin(t)$.

The hyperchaotic attractors of the resulting system (6) are depicted in figure 12. Numerical results for GFPS between the transmitter and receiver systems via the controllers (13) and the parameter update rule (14) and its application to secure communication are illustrated in figure 13. Figure 13(a) describes the time evolution of the synchronization errors $e_i$ ($i = 1,2,3,4,5$), which shows that the time response of the errors approach the origin very fast. So the desired synchronization is obtained. The original message signal $s(t)$ and the recovered one $\hat{s}(t)$ are plotted in figures 13(b) and (c), respectively. Figure 13(d) displays the error signal $\hat{s}(t) - s(t)$ between the message signal $s(t)$ and the recovered one $\hat{s}(t)$. As seen, the signal error tends to zero in a very short time. Thus, the message signal is recovered accurately.

## 5. Conclusion

This paper presents a new 5D hyperchaotic system generated from the Lü hyperchaotic system. Some basic dynamical behaviors of the system are explored by investigating its Lyapunov exponents spectrum and bifurcation diagrams. And various phase portraits of the system has been demonstrated by computer simulations. Furthermore, combining GFPS of the new 5D hyperchaotic system with the parameter modulation technique, we have introduced a new chaotic secure communication method. In contrast to existing chaotic secure communication approaches, there are no limitations on the message size in our scheme. Under this structure, the message signal can successfully and secretly be transmitted through four main functions, i.e., modulation, chaotic transmitter, chaotic receiver and demodulation. Finally, numerical simulations have been provided to verify the effectiveness and the feasibility of the presented secure communication scheme.

## Acknowledgments

This research was jointly supported by the National Natural Science Foundation of China (Grant Nos. 61004006 and 61203094), China Postdoctoral Science Foundation (Grant No. 2013M530181), the Natural Science Foundation of Henan Province, China (Grant No. 13230010254), Program for Science & Technology Innovation Talents in Universities of Henan Province, China (Grant No. 14HASTIT042), the Foundation for University Young Key Teacher Program of Henan Province, China (Grant No. 2011GGJS-025), Shanghai Postdoctoral Scientific Program (Grant No. 13R21410600), the Science & Technology Project Plan of Archives Bureau of Henan Province (Grant No. 2012-X-62) and the Natural Science Foundation of Educational Committee of Henan Province, China (Grant No. 13A520082). The authors would like to thank the anonymous reviewers and the editor for their helpful comments.

## References


[1] Perez G and Cerdeira H A 1995 Extracting messages masked by chaos *Phys. Rev. Lett.* **74** 1970–3

[2] Li Y X, Chen G and Tang W K S 2005 Controlling a unified chaotic system to hyperchaotic *IEEE Trans. Circuit Syst.* II **52** 204–7

[3] Li Y X, Tang W K S and Chen G R 2005 Generating hyperchaos via state feedback control *Int. J. Bifurcation Chaos* **15** 3367–75

[4] Jia Q 2007 Generation and suppression of a new hyperchaotic system with double hyperchaotic attractors *Phys. Lett.* A **371** 410–5

[5] Niu Y, Wang X, Wang M and Zhang H 2010 A new hyperchaotic system and its circuit implementation *Commun. Nonlinear Sci. Numer. Simul.* **15** 3518–24

[6] Chen C H, Sheu L J, Chen H K, Chen J H, Wang H C, Chao Y C and Lin Y K 2009 A new hyper-chaotic system and its synchronization *Nonlinear Anal. RWA* **10** 2088–96

[7] Zheng S, Dong G and Bi Q 2010 A new hyperchaotic system and its synchronization *Appl. Math. Comput.* **215** 3192–200

[8] Chen Z, Yang Y, Qi G and Yuan Z 2007 A novel hyperchaos system only with one equilibrium *Phys. Lett.* A **360** 696–701

[9] Pecora L M and Carroll T L 1990 Synchronization in chaotic systems *Phys. Rev. Lett.* **64** 821–4

[10] Li Z G and Xu D L 2004 A secure communication scheme using projective chaos synchronization *Chaos Solitons Fractals* **22** 477–81

[11] Uyaroğlu Y and Pehlivan Ī 2010 Nonlinear sprott94 case a chaotic equation: synchronization and masking communication applications *Comput. Electr. Eng.* **36** 1093–100

[12] Wu X, Wang H and Lu H 2012 Modified generalized projective synchronization of a new fractional-order hyperchaotic system and its application in secure communication *Nonlinear Anal. RWA* **13** 1441–50

[13] Cheng C J 2012 Robust synchronization of uncertain unified chaotic systems subject to noise and its application to secure communication *Appl. Math. Comput.* **219** 2698–712

[14] Boccaletti S, Bianconi G, Criado R, del Genio C I, Gómez-Gardeñes J, Romance M, Sendiña-Nadal I, Wang Z and Zanin M 2014 The structure and dynamics of multilayer networks *Phys. Rep.* **544** 1–122

[15] Wang Z, Wang L and Matjaž P 2014 Degree mixing in multilayer networks impedes the evolution of cooperation *Phys. Rev.* E **89** 052813

[16] Zheng Z G and Hu G 2000 Generalized synchronization versus phase synchronization *Phys. Rev.* E **62** 7882–5

[17] Rosenblum M G, Pikovsky A S and Kurths J 1996 Phase synchronization of chaotic oscillators *Phys. Rev. Lett.* **76** 1804–7

[18] Pikovsky A S, Rosenblum M G and Kurths J 1997 From phase to lag synchronization in coupled chaotic oscillators *Phys. Rev. Lett.* **78** 4193–7

[19] Chen Y and Li X 2007 Function projective synchronization between two identical chaotic systems *Int. J. Mod. Phys.* C **18** 883–8

[20] Luo R Z 2008 Adaptive function project synchronization of Rössler hyperchaotic system with uncertain parameters *Phys. Lett.* A **372** 3667–71

[21] Du H Y, Zeng Q S and Wang C H 2008 Function projective synchronization of different chaotic systems with uncertain parameters *Phys. Lett.* A **372** 5402–10

[22] Du H, Zeng Q and Wang C 2009 Modified function projective synchronization of chaotic system *Chaos Solitons Fractals* **42** 2399–404

[23] Yu Y and Li H 2010 Adaptive generalized function projective synchronization of uncertain chaotic systems *Nonlinear Anal. RWA* **11** 2456–64

[24] Fallahi K and Leung H 2010 A chaos secure communication scheme based on multiplication modulation *Commun. Nonlinear Sci. Numer. Simul.* **15** 368–83

[25] Bocaletti S, Kurths J, Osipov G, Valladares D and Zhou C 2002 The synchronization of chaotic systems *Phys. Rep.* **366** 1–101

[26] Megam Ngouonkadi E B, Fotsin H B and Louodop Fotso P 2014 Implementing a memristive Van der Pol oscillator coupled to a linear oscillator: synchronization and application to secure communication *Phys. Scr.* **89** 035201

[27] Lin J S, Huang C F, Liao T L and Yan J J 2010 Design and implementation of digital secure communication based on synchronized chaotic systems *Digit. Signal Process.* **20** 229–37

[28] Wu X J, Wang H and Lu H T 2011 Hyperchaotic secure communication via generalized function projective synchronization *Nonlinear Anal. RWA* **12** 1288–99

[29] Dedieu H, Kennedy M P and Hasler M 1993 Chaos shift keying: modulation and demodulation of a chaotic carrier using self-synchronizing Chua's circuits *IEEE Trans. Circuit Syst.* II **40** 634–42

[30] Hou Y Y, Chen H C, Chang J F, Yan J J and Liao T L 2012 Design and implementation of the Sprott chaotic secure digital communication systems *Appl. Math. Comput.* **218** 11799–805

[31] Mahmoud G M, Mahmoud E E and Arafa A A 2013 On projective synchronization of hyperchaotic complex nonlinear systems based on passive theory for secure communications *Phys. Scr.* **87** 055002

[32] Liu S and Zhang F 2014 Complex function projective synchronization of complex chaotic system and its applications in secure communication *Nonlinear Dyn.* **76** 1087–97

[33] Chen A M, Lu J A, Lü J H and Yu X M 2006 Generating hyperchaotic Lü attractor via state feedback control *Physica* A **364** 103–10

[34] Wolf A, Swift J B, Swinney H L and John A W 1985 Determining Lyapunov exponents from a time series *Physica* D **16** 285–317

[35] Volder J E 1959 The CORDIC trigonometric computing technique *IRE Trans. Electron. Comput.* **EC-8** 330–4

[36] Meher P K, Valls J, Juang T B, Sridharan K and Maharatna K 2009 50 Years of CORDIC: algorithms, architectures, and applications *IEEE Trans. Circuit Syst.* I **56** 1893–907

[37] Hu X, Harber R G and Bass S C 1991 Expanding the range of convergence of the CORDIC algorithm *IEEE Trans. Comput.* **40** 13–21

[38] Andraka R 1998 A survey of CORDIC algorithms for FPGA based computers *Proc. 6th ACM/SIGDA Int. Symp. on Field Programmable Gate Arrays (FPGA'98)* pp 191–200

[39] Parhi K K 1999 *VLSI Digital Signal Processing Systems: Design and Implementation* (New York: Wiley)

[40] Antelo E, Lang T and Bruguera J D 2000 Very-high radix circular CORDIC: vectoring and unified rotation/vectoring *IEEE Trans. Comput.* **49** 727–39

[41] Antelo E and Villalba J 2005 Low latency pipelined circular CORDIC *Proc. 17th IEEE Symp. on Comput. Arithm.* pp 280–7